

PACS numbers: 78.67.–n; 68.65.–k; 42.25.Fx
DOI: 10.1070/QE2010v040n11ABEH014330

Microscopic theory of optical properties of composite media with chaotically distributed nanoparticles

A.S. Shalin

Abstract. **The boundary problem of light reflection and transmission by a film with chaotically distributed nanoinclusions is considered. Based on the proposed microscopic approach, analytic expressions are derived for distributions inside and outside the nanocomposite medium. Good agreement of the results with exact calculations and (at low concentrations of nanoparticles) with the integral Maxwell-Garnett effective-medium theory is demonstrated. It is shown that at high nanoparticle concentrations, averaging the dielectric constant in volume as is done within the framework of the effective-medium theory yields overestimated values of the optical film density compared to the values yielded by the proposed microscopic approach. We also studied the dependence of the reflectivity of a system of gold nanoparticles on their size, the size dependence of the plasmon resonance position along the wavelength scale, and demonstrated a good agreement with experimental data.**

Keywords: *metamaterial, chaotic nanocomposite, scattering of light by small particles, effective-medium theory.*

1. Introduction

At present, of great interest are investigations of different low-dimensional objects as well as systems consisting of these objects (colloids, composites, photonic crystals, etc. [1–4]) or systems with nano- and micro-inhomogeneities (micro- and mesoporous structures [5, 6]). Indeed, by varying material and geometrical parameters of such structures, it is possible to obtain, for example, a medium with a giant, superlow, negative, or unit refractive index [7–10] and to increase the optical transparency of metal films and layers [11–13]. Maxwell-Garnett [14] was first to put forward the idea that nanoaggregates organised in a proper way can have unusual optical properties. This effect is explained by the presence of a field reradiated by 'foreign' inclusions [10, 15, 16], the field leading to additional polarisation of medium molecules, which affects the macroscopic optical properties of the medium itself. However, the Maxwell-Garnett effective-medium method and its modifications (Bruggeman, Clausius–Mosotti, etc.) have a small applicability domain because they take into account only electrostatic interaction of nanoinclusions. As is shown in monographs [17, 18] such an approximation is insufficient to describe adequately the systems where the effects of coherent scattering, interference of the field scattered by nanoparticles, delay of electrodynamic interaction play a key role as well as when the field is inhomogeneous in the nanoparticle volume. In fact, effective-medium approximation is applicable only in a rather narrow interval of geometric and material parameters of a composite or colloid when the interparticle distance in the mentioned systems is sufficiently large to neglect the multipolar components of the field scattered by nanoparticles as well as the interaction of nonadjacent particles. Nonetheless, it should be emphasised that these approaches, even beyond the mentioned restrictions, can be used for evaluative research [10]. For instance, Moiseev et al. [19] showed that away from the plasmon resonance of metal nanoclusters the Maxwell-Garnett theory (compared to the exact numerical calculations by the finite element method) describes well the optical properties of a single-layer ordered metal-dielectric nanocomposite representing a square lattice made of clusters.

In this paper, we propose a method based on formalism of integral equations, which we previously used to study different nanoaggregates (for example, dimers and chains of interacting nanoclusters [7, 20], an ordered single-layer of nanoparticles on a substrate surface [4, 21], an ordered nanocrystal composite [22]) as well as based on the quasi-regular approximation which we will describe below. The method allows one to investigate the optical properties of a colloid nanoaggregate in the interval of material and geometric parameters where the conventional effective-medium theories either yield a large error or become inapplicable. Because the proposed method uses a microscopic rather than a medium-volume-averaged field, we can take into account the dimensional and structural factors of a system of nanoparticles, study quasi-ordered aggregates or aggregates with defective nanocrystal structures (both periodic and chaotic), etc. Note also that it is possible to examine the effective parameters of each particle.

The advantage of this method compared to exact methods (finite element method [23], FDTD method [24, 25], coupled dipole method [26], etc.) is its higher computation speed. Moreover, to employ the above methods requires a strictly specified geometry of the system; therefore, investigation of a chaotic aggregate necessitates averaging over a set of numerical experiments with different geometries [27], which complicates markedly the computation. In this connection, exact methods are rarely used to calculate the optical parameters of chaotic aggregates; therefore, the refinement of the effective-medium theory or development of an alternative 'fast' method is urgent.

A.S. Shalin Ul'yanovsk State University, ul. L. Tolstogo 42, 432700 Ul'yanovsk, Russia; Ulyanovsk Branch, V.A. Kotel'nikov Institute of Radioengineering and Electronics, Russian Academy of Sciences, ul. Goncharova 48, 432011 Ul'yanovsk, Russia;
e-mail: shalin_a@rambler.ru

Received 1 April 2010; revision received 13 September 2010
Kvantovaya Elektronika **40** (11) 1004–1011 (2010)
Translated by I.A. Ulitkin

2. Basic equations

According to the integral equation method [28] which we used many times to study different nanoaggregates [7, 21, 22], the field produced by a composite medium at each point of the space can be written in the form:

$$\boldsymbol{E}(\boldsymbol{r},t) = \boldsymbol{E}_{\text{in}}(\boldsymbol{r},t) + \int_V \operatorname{curl}\operatorname{curl}\frac{\boldsymbol{P}(\boldsymbol{r}',t-R/c)}{R}\mathrm{d}V'$$

$$+\frac{3}{4\pi}\sum_{j=1}^{J}\int_{V_j}\operatorname{curl}\operatorname{curl}\frac{N_j\,\alpha_j\,\boldsymbol{E}'_{j\,\text{eff}}(\boldsymbol{r}'_j,t-R'_j/c)}{R'_j}\mathrm{d}V'_j, \qquad (1)$$

where $\boldsymbol{E}_{\text{in}}(\boldsymbol{r},t) = \boldsymbol{E}_{0\,\text{in}}\exp(\mathrm{i}\boldsymbol{k}_0\boldsymbol{r} - \mathrm{i}\omega t)$ is an external wave at the observation point $\boldsymbol{r}$; $\boldsymbol{k}_0$ is the wave vector; the first integral determines the field produced by the $\boldsymbol{P}$-polarised medium-matrix, proportional to the field incident on the medium surface, and by the dielectric constant $\tilde{\varepsilon}_{\text{m}}$; $R = |\boldsymbol{r} - \boldsymbol{r}'|$ is the distance from the integration point $\boldsymbol{r}'$ located inside the medium to the observation point; V is the medium volume; c is the speed of light in vacuum; the argument $(t - R/c)$ characterises the delay of the corresponding quantity. The third term in the right hand part of (1) defines the field generated directly by J interacting nanoparticles of volume V_j consisting of atoms with polarisability α_j and concentration N_j; $R_j = |\boldsymbol{r} - \boldsymbol{r}'_j|$; $\boldsymbol{r}'_j$ is the point of integration inside the jth nanoparticle with respect to the coordinate origin. The field $\boldsymbol{E}'_{j\text{eff}}$ in expression (1) differs from the field $\boldsymbol{E}_{\text{in}}$ of the incident plane wave and represents a wave affecting each point inside the jth nanoparticle with account for all the fields reradiated by the atoms of all nanoparticles. We will call this field effective. In this case, $\boldsymbol{E}'_{j\text{eff}}$ has two components, according to [28]: external – acting from surroundings and internal – determining the interaction of atoms inside the nanoparticle and responsible for formation of the permittivity of the medium. Account for the internal field divides equation (1) into local and nonlocal (described in detail in [28]), the first one being reduced to the known Lorentz–Lorenz equation:

$$\frac{4\pi}{3}N_j\,\alpha_j = \frac{\tilde{\varepsilon}_j(\boldsymbol{r}'_j) - \tilde{\varepsilon}_{\text{m}}}{\tilde{\varepsilon}_j(\boldsymbol{r}'_j) + 2\tilde{\varepsilon}_{\text{m}}},$$

where $\tilde{\varepsilon}_j(\boldsymbol{r}'_j)$ is the complex dielectric constant of nanoparticles. The formulated problem is thus reduced to the solution of nonlocal equations and to a search for effective fields $\boldsymbol{E}_{j\text{eff}}$ incident on nanoparticles from the surroundings.

We will consider a composite consisting of identical homogeneous spherical nanoclusters (radii, $a_j = a_i = a$; dielectric constants, $\tilde{\varepsilon}_j(\boldsymbol{r}) = \tilde{\varepsilon}_i(\boldsymbol{r}) = \tilde{\varepsilon}$) and use the long-wave approximation [18] specified by the conditions

$$k_0 a \ll 1,\ k_0 n a \ll 1 \qquad (2)$$

($n = \sqrt{\tilde{\varepsilon}}$ is the refractive index of a nanoparticle), which mean that the strengths $\boldsymbol{E}_{\text{in}}$ and $E_{j\text{eff}}$ weakly change in the cluster volume. We will restrict our consideration within this work by the case when the vectors of the particle and medium polarisations are the linear functions of the field strength. Placing the observation point and the coordinate origin on the medium-matrix surface, we will write the effective field at the centre of the ith particle in the form (1):

$$\boldsymbol{E}_{i\,\text{eff}}(\boldsymbol{r}_i) = \frac{3}{4\pi}\frac{\tilde{\varepsilon} - \tilde{\varepsilon}_{\text{m}}}{\tilde{\varepsilon} + 2\tilde{\varepsilon}_{\text{m}}}$$

$$\times\sum_{j=1,\,j\neq i}^{J}\int_{V_j}\operatorname{curl}\operatorname{curl}\frac{\boldsymbol{E}_{j\,\text{eff}}\left[\boldsymbol{r}'_j, t - |\boldsymbol{r}_i - \boldsymbol{r}'_j|/(c/\tilde{n}_{\text{m}})\right]}{|\boldsymbol{r}_i - \boldsymbol{r}'_j|}\mathrm{d}V'_j$$

$$+(\hat{G}\boldsymbol{E}_{\text{in}}(0))\exp(\mathrm{i}\boldsymbol{k}_0\boldsymbol{r}_i\tilde{n}_{\text{m}}), \qquad (3)$$

where $\tilde{n}_{\text{m}} = \sqrt{\tilde{\varepsilon}_{\text{m}}}$ is the refractive index of the medium-matrix, and the first term in the right hand part is a superposition of the fields generated by aggregate nanoparticles at the centre of the ith nanocluster. In this case, we take into account that the waves produced by the particles propagate at a velocity $c/\tilde{n}_{\text{m}}$. The second term with the tensor $\hat{G}$ determines the field generated by the matrix atoms at a point corresponding to the centre of the ith particles when the medium-matrix is continuous and does not contain nanoinclusions. In fact, the term responsible for the external field and the integral in (1) describing the field produced by a pure medium (in the absence of nanoparticles) are reduced (according to the extinction theorem) to a tensor of Fresnel transmission coefficients in the case of a semi-infinite medium and to a tensor of Airy coefficients for the fields inside the film in the case of a film [28].

Thus, having solved the system of J equations (3) in the general form, we obtain the values of the effective fields at the centre of each nanoparticle. The field reflected from the composite will take the form according to (1)–(3):

$$\boldsymbol{E}_{\text{refl}}(\boldsymbol{R}) = \frac{3}{4\pi}\frac{\tilde{\varepsilon} - \tilde{\varepsilon}_{\text{m}}}{\tilde{\varepsilon} + 2\tilde{\varepsilon}_{\text{m}}}$$

$$\times\sum_{j=1}^{J}\int_{V_j}\operatorname{curl}\operatorname{curl}\frac{\boldsymbol{E}_{j\,\text{eff}}(\boldsymbol{r}'_j, t - |\boldsymbol{R} - \boldsymbol{r}'_j|/c')}{|\boldsymbol{R} - \boldsymbol{r}'_j|}\mathrm{d}V'_j$$

$$+(\hat{R}\boldsymbol{E}_{\text{in}}(0))\exp(\mathrm{i}\boldsymbol{k}_0\boldsymbol{R}), \qquad (4)$$

where $\hat{R}$ is the tensor of the reflection coefficients; $\boldsymbol{R}$ is the radius vector of the observation point. In this case, we have $c' = c/\tilde{n}_{\text{m}}$ on the interval where the wave scattered by a nanoparticles moves from the particle to the medium-matrix surface, and $c' = c$ on the interval from the surface to the observation point.

3. Electromagnetic fields inside the composite

Consider a field generated by the jth nanoparticle at some observation point $\boldsymbol{R}$ outside its volume. The integral corresponding to the strength in (1) can be easily found in the long-wave approximation by the Ewald–Ozeen method [28], which was previously done in papers [15, 20]. As a result, we obtained the relations:

$$\boldsymbol{E}_{j\,\text{sca}}(\boldsymbol{R}) = \alpha_{\text{p}}\hat{f}_j(R)\boldsymbol{E}_{j\,\text{eff}},\ \ \alpha_{\text{p}} = a^3\frac{\tilde{\varepsilon} - \tilde{\varepsilon}_{\text{m}}}{\tilde{\varepsilon} + 2\tilde{\varepsilon}_{\text{m}}}, \qquad (5)$$

where the tensor $\hat{f}_j(R)$ has the components corresponding to the parallel and perpendicular external-field polarisations with respect to $\boldsymbol{R}$ [18, 28]:

$$f_j^{\mathrm{P}}(R) = \exp(\mathrm{i}k_0\tilde{n}_{\mathrm{m}}R)\left(\frac{2}{R^3} - \frac{2\mathrm{i}k_0\tilde{n}_{\mathrm{m}}}{R^2}\right),$$

$$f_j^{\mathrm{S}}(R) = \exp(\mathrm{i}k_0\tilde{n}_{\mathrm{m}}R)\left[-\frac{1}{R^3} + \frac{\mathrm{i}k_0\tilde{n}_{\mathrm{m}}}{R^2} + \frac{(k_0\tilde{n}_{\mathrm{m}})^2}{R}\right]. \quad (6)$$

Note that it is necessary to take into account the higher-order multipoles in expansion (6) only when the interparticle distance (distance between the particle centres) is shorter than $2.1a$ or when condition (2) is violated because in the opposite case the multipolar components make an insignificant contribution to the field scattered by interaction nanoparticles, this fact being confirmed by detailed research in paper [29]. The number of so closely packed clusters becomes statistically significant only when their concentration is very high and close to that of densely packed nanoparticles, which are described by the methods developed in the theory of photonic crystals [17, 30]. In this paper, we will restrict our consideration to systems where the nanoparticle concentration is such that it allows one to limit expansion (6) by dipole components.

After transforming the integral terms in (3), (4) in accordance with (5), (6), we obtain a system of linear equations for the field incident on a cluster (3):

$$\boldsymbol{E}_{i\,\mathrm{eff}}(\boldsymbol{r}_i) = \alpha_{\mathrm{p}} \sum_{j=1,\,j\neq i}^{J} \hat{f}_j(|\boldsymbol{r}_i - \boldsymbol{r}_j|)\boldsymbol{E}_{j\,\mathrm{eff}} + (\hat{G}\boldsymbol{E}_{\mathrm{in}}(0))\exp(\mathrm{i}\boldsymbol{k}_0\boldsymbol{r}_i\tilde{n}_{\mathrm{m}}); \quad (7)$$

expression (4) is also linearised to the form

$$\boldsymbol{E}_{\mathrm{refl}}(\boldsymbol{R}) = \alpha_{\mathrm{p}} \sum_{j=1}^{J} \hat{f}_j'(|\boldsymbol{R} - \boldsymbol{r}_j|)\boldsymbol{E}_{j\,\mathrm{eff}} + (\hat{R}\boldsymbol{E}_{\mathrm{in}}(0))\exp(\mathrm{i}\boldsymbol{k}_0\boldsymbol{R}), \quad (8)$$

where $\hat{f}'$ depends on the above determined c'.

4. Lattice sums. Quasi-regular approximation

Solution of the system of equations (7) and calculation of (8) seem, at first sight, to be rather simple numerical problems, but they are difficult to realise. This is explained by the presence of long-range terms ($\sim 1/R$) in the particle interaction tensor (6), which lead to poor convergence of mentioned sums as was repeatedly noticed by different authors [17, 31, 32]. Indeed, because the number J of particles in a macroscopic object tends to infinity and it is impossible to neglect the influence of remote particles in the limelight of the aforesaid, we will have an infinite number of equations in systems (3) and (7). However, there exist ways to overcome this difficulty.

One of the most widely used methods for calculating lattice sums is the so-called Lorentz method according to which nanoparticles in the vicinity of the observation point can be considered to be discretely distributed, while distant nanoparticles can be considered to be continuously distributed and their effect can be taken into account iby integrating over the entire volume. This approach, as was shown in [10] leads to the Maxwell-Garnett effective-medium theory at small concentrations.

On the other hand, as was noted in paper [33], in some cases the results obtained by the Lorentz method strongly disagree with the exact calculations by the coupled dipole method

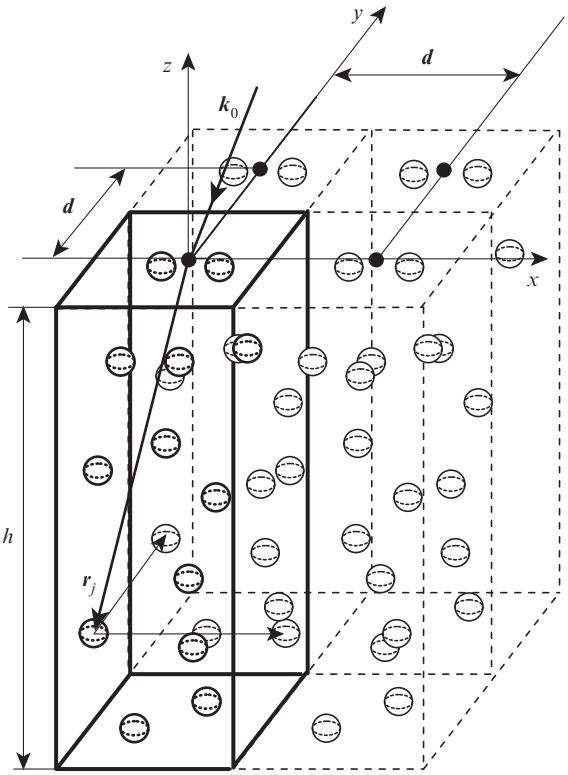

Figure 1. Representation of a chaotic system in the form of a quasi-regular aggregate by translating the domain with characteristic dimensions h and d and a translation constant d.

[34]. In this connection, we suggest using the so-called quasi-regular approximation [27], which allows one to employ the Ewald method to calculate the sums in crystal lattices [4, 31, 35, 36]. The approximation implies that a chaotic aggregate can be presented in the form of some periodic (with a period d) structure (Fig. 1) consisting of identical domains with chaotically distributed nanoparticles. Thus, the entire composite is divided into two parts: chaotically distributed nanoparticles interacting within one domain and a periodic structure affecting the nanoparticles:

$$\boldsymbol{E}_{i\,\mathrm{eff}}(\boldsymbol{r}_i) = \alpha_{\mathrm{p}}\left\{\sum_{j=1,\,j\neq i}^{S} \hat{f}_j(|\boldsymbol{r}_i - \boldsymbol{r}_j|)\boldsymbol{E}_{j\,\mathrm{eff}} + \sum_{j=1}^{S}\left[\sum_{b=-\infty,\,b\neq 0}^{\infty} \hat{f}_j(|\boldsymbol{r}_i - (\boldsymbol{r}_j + \boldsymbol{d}b)|)\exp(\mathrm{i}\boldsymbol{q}\boldsymbol{r}_b)\right]\boldsymbol{E}_{j\,\mathrm{eff}}\right\} + (\hat{G}\boldsymbol{E}_{\mathrm{in}}(0))\exp(\mathrm{i}\boldsymbol{k}_0\boldsymbol{r}_i\tilde{n}_{\mathrm{m}}), \quad (9)$$

$$\boldsymbol{E}_{\mathrm{refl}}(\boldsymbol{R}) = \alpha_{\mathrm{p}}\sum_{j=1}^{S}\left[\sum_{b=-\infty}^{\infty} \hat{f}_j'(|\boldsymbol{R} - (\boldsymbol{r}_j + \boldsymbol{d}b)|)\exp(\mathrm{i}\boldsymbol{q}\boldsymbol{r}_b)\right]\boldsymbol{E}_{j\,\mathrm{eff}} + (\hat{R}\boldsymbol{E}_{\mathrm{in}}(0))\exp(\mathrm{i}\boldsymbol{k}_0\boldsymbol{R}), \quad (10)$$

where $\boldsymbol{r}_{\mathrm{b}}$ is the radius vector of the central point of the upper face of the bth domain (zero point of the bth domain, Fig. 1). The number of particles in the domain S and accordingly the

number of domains is assumed equal to infinity. We also allow for the condition of parallel translation symmetry [35, 36]

$$\boldsymbol{E}_{\text{inc}}(\boldsymbol{r}_b) = \boldsymbol{E}_{\text{inc}}(0)\exp(\mathrm{i}\boldsymbol{q}\boldsymbol{r}_b),$$

taking into account the phase difference of the field that is incident on nanoparticles belonging to different domains, whether it be external wave or wave scattered by any particle. In this case, the vector $\boldsymbol{q}$ has components $(q_x, q_y, 0)$, where $q_x = k_0\tilde{n}_{\text{m}}\sin\theta_{\text{in}}\cos\varphi$; $q_y = k_0\tilde{n}_{\text{m}}\sin\theta_{\text{in}}\sin\varphi$; θ_{in} is the angle of incidence; φ is the angle between the coordinate axis x and the plance of incidence. Summation in j is performed inside one domain, and b is an index of summation in the domains. Because the domains are in identical conditions, $|\boldsymbol{E}_{j\text{eff}}|$ for different b are equal and the phase multiplier is determined by the principle of parallel translation symmetry.

Thus, the number of equations decreases down to the number S of particles in the domain. In this case, the field of each of them corresponds to a wave generated by an ordered periodic infinite layer of nanoparticles rather than by one isolated cluster. Because the position of nanoparticles in the domain is chaotic, the corresponding single-layers are randomly displaced with respect to each other.

Obviously, passage to an ordered nanoaggregate or a partially ordered aggregate is not difficult here – it is only necessary to appropriety specify the coordinates of the particle centres and domain parameters based on the presumed geometric parameters of the composite. This can be useful for the theory of photonic crystals and for studying the effect of nanoinclusions on the band-gap structure of the latter [30, 37].

We will use the Ewald method to calculate the lattice sums in (9), (10).

Consider first the case when the observation point $\boldsymbol{r}$ is outside the single layer under study. Because the function describing the nanoparticle field is periodic with a period of domain location, it can be expanded in a Fourier series over the vectors of the inverse lattice. Derivation of the mentioned expressions can be found in papers [35, 36]. We will write here the result:

$$\hat{C}_p(\boldsymbol{r}-\boldsymbol{r}_j) = \sum_{b=-\infty}^{\infty}\hat{f}_j(|\boldsymbol{r}-(\boldsymbol{r}_j+\boldsymbol{d}b)|)\exp(\mathrm{i}\boldsymbol{q}\boldsymbol{r}_b)$$
$$= \sum_{p,q=-\infty}^{\infty}\boldsymbol{A}_{pq}(\boldsymbol{r})\exp(\mathrm{i}\boldsymbol{q}\boldsymbol{r}_b), \tag{11}$$

$$\boldsymbol{A}_{pq}(\boldsymbol{r}) = -\frac{2\pi\mathrm{i}}{|\boldsymbol{a}_1\times\boldsymbol{a}_2|}[\boldsymbol{k}_{pq}\times(\boldsymbol{k}_{pq}\times\boldsymbol{n}_0)]$$
$$\times\frac{\exp[\mathrm{i}(\boldsymbol{k}_{pq}-\boldsymbol{q})(\boldsymbol{r}-\boldsymbol{r}_j)]}{\kappa_{pq}}, \tag{12}$$

where $\boldsymbol{n}_0 = \boldsymbol{E}_{\text{in}}/|\boldsymbol{E}_{\text{in}}|$;

$$\boldsymbol{k}_{pq} = \begin{cases}\boldsymbol{q}+\boldsymbol{g}^{\parallel}_{pq}, \kappa_{pq}, & z>0,\\ \boldsymbol{q}+\boldsymbol{g}^{\parallel}_{pq}, -\kappa_{pq}, & z<0;\end{cases} \tag{13}$$

$$\kappa_{pq} = \sqrt{k_0^2-(\boldsymbol{q}+\boldsymbol{g}^{\parallel}_{pq})^2};\ \boldsymbol{g}^{\parallel}_{pq} = p\boldsymbol{g}_1+q\boldsymbol{g}_2; \tag{14}$$

$$\boldsymbol{g}_1 = 2\pi\frac{\boldsymbol{a}_2\times\boldsymbol{n}}{|\boldsymbol{a}_1\times\boldsymbol{a}_2|},\ \boldsymbol{g}_2 = 2\pi\frac{\boldsymbol{n}\times\boldsymbol{a}_1}{|\boldsymbol{a}_1\times\boldsymbol{a}_2|}$$

are the inverse lattice vectors; $\boldsymbol{a}_1 = (d,0,0)$, $\boldsymbol{a}_2 = (0,d,0)$ are the direct-lattice translation vectors of the domains chosen from the considerations of their minimal length, and the vector $\boldsymbol{n} = (0,0,1)$ is perpendicular to the medium surface.

Expression (11) is an expansion of the field (produced by a domain lattice) in a plane harmonic wave ($p = q = 0$) and in a series of exponentially decaying evanescent waves taking place at $|\boldsymbol{q}+\boldsymbol{g}_{pq}| > k_0$, when κ_{pq} is imaginary.

Let us calculate now the lattice sum for the observation points inside the single layer, the sum describing mutual interaction of nanoparticles belonging to the layer. Following the Ewald method [32, 35], we will write the expression

$$\hat{A}_{\text{p}} = \sum_{b=-\infty, b\neq 0}^{\infty}\hat{f}_j(|\boldsymbol{r}_i-(\boldsymbol{r}_j+\boldsymbol{d}b)|)\exp(\mathrm{i}\boldsymbol{q}\boldsymbol{r}_b)$$
$$= \hat{l}(\boldsymbol{k}_0)\boldsymbol{n}_0\exp(\mathrm{i}\boldsymbol{q}\boldsymbol{r}_b). \tag{15}$$

The tensor $\hat{l}$ is a symmetric tensor with zero components l_{xz}, l_{yz}, l_{zx}, l_{zy} and has the form:

$$l^{\mu\nu}(\boldsymbol{k}_0) = c^{\mu\nu}+\left[\frac{2}{3}\mathrm{i}k_0^3\mathrm{Erfc}\left(-\frac{\mathrm{i}k_0}{2F}\right)\right.$$
$$\left.+\frac{4F}{3\sqrt{\pi}}(k_0^2-F^2)\exp\left(\frac{k_0^2}{4F^2}\right)-\frac{2}{3}\mathrm{i}k_0^3\right]\delta^{\mu\nu}. \tag{16}$$

where $\delta^{\mu\nu}$ is the Kronecker delta.

In expression (16), the term $-{}^2/_3\mathrm{i}k_0^3$ takes into account the radiative decay, and

$$c^{\mu\nu} = \frac{\mathrm{i}\pi}{|\boldsymbol{a}_1\times\boldsymbol{a}_2|}\sum_{p,q}\left[\frac{k_0^2\delta^{\mu\nu}-k_{pq\nu}k_{pq\mu}}{\kappa_{pq}}\Delta_{pq}(1+\tau)+\eta_0\Sigma_{pq}\right]$$
$$+\frac{1}{2}\sum_{n,m}\frac{\exp(\mathrm{i}\boldsymbol{k}_0\boldsymbol{a}_{nm})}{a_{nm}^3}\{\Gamma^{(1)}_{nm}[\delta^{\mu\nu}\Gamma^{(2)}_{nm}+\boldsymbol{a}^{\mu}_{nm}\boldsymbol{a}^{\nu}_{nm}\Gamma^{(3)}_{nm}]$$
$$+\Gamma^{(4)}_{nm}[-\delta^{\mu\nu}a_{nm}+\boldsymbol{a}^{\mu}_{nm}\boldsymbol{a}^{\nu}_{nm}\Gamma^{(5)}_{nm}]\}, \tag{17}$$

where $\mu,\nu = x,y,z$; $\boldsymbol{a}_{nm} = n\boldsymbol{a}_1+m\boldsymbol{a}_2$; $a_{nm} = |\boldsymbol{a}_{nm}|$; n, m are integers;

$$\eta_0 = \delta^{\mu z}\delta^{\nu z};\ \tau = (-1)^{\delta^{\mu z}}(-1)^{\delta^{\nu z}};$$
$$\Delta_{pq} = \mathrm{Erfc}\left(-\frac{\mathrm{i}k_{pq}}{2F}\right);\ \Sigma_{pq} = \frac{\mathrm{i}4F}{\sqrt{\pi}}\exp\left(\frac{k_{pq}^2}{4F^2}\right);$$
$$\Gamma^{(1)}_{nm} = \exp(-\mathrm{i}k_0a_{nm})\mathrm{Erfc}\left(a_{nm}F-\frac{\mathrm{i}k_0}{2F}\right);$$
$$\Gamma^{(2)}_{nm} = -1-\mathrm{i}k_0a_{nm}+k_0^2a_{nm}^2; \tag{18}$$
$$\Gamma^{(3)}_{nm} = -k_0^2+\frac{3\mathrm{i}k_0}{a_{nm}}+\frac{3}{a_{nm}^2};$$
$$\Gamma^{(4)}_{nm} = \frac{2F}{\sqrt{\pi}}\exp\left(-F^2a_{nm}^2+\frac{k_0^2}{4F^2}\right);$$
$$\Gamma^{(5)}_{nm} = \frac{3}{a_{nm}}+2F^2a_{nm};\ F = \sqrt{\pi/|\boldsymbol{a}_1\times\boldsymbol{a}_2|}.$$

The convergence of sums in (16) is determined by the parameter F, which has the dimensionality of reciprocal

length. This parameter has no physical sense and should be a real positive quantity. Substituting F into (18), we can find the maximal values of subscripts m, n and p, q needed to calculate the lattice sums with the given accuracy. Taking into account the fact that at large arguments $\mathrm{Erfc}(x) = \exp(-x^2)/(x\sqrt{\pi})$, we obtain the condition:

$$\exp(-\pi a_{nm}^2/|\boldsymbol{a}_1\times\boldsymbol{a}_2|) \approx \xi, \tag{19}$$

where ξ is a small quantity determining the calculation accuracy. An exact numerical calculation for a square lattice shows that a change in the subscripts m, n and p, q from –2 to 2 ensures a relative accuracy of 10^{-6} in calculating the lattice sums, in agreement with the estimate from (19).

5. Optical characteristics of a composite system

Substituting (11) and (15) into (9) and (10), as well as taking into account that the amplitudes $\boldsymbol{E}_{j\mathrm{eff}}$ are equal at different b, for the effective fields inside the particles and for the field produced by the medium as a whole, we will write the final expressions in the form:

$$\boldsymbol{E}_{i\mathrm{eff}}(\boldsymbol{r}_i) = \alpha_\mathrm{p}\left[\sum_{j=1,\,j\neq i}^{S}\hat{C}_\mathrm{p}^{\pm}(\boldsymbol{r}_i-\boldsymbol{r}_j)\boldsymbol{E}_{j\mathrm{eff}}(\boldsymbol{r}_j)+\hat{A}_\mathrm{p}\boldsymbol{E}_{i\mathrm{eff}}(\boldsymbol{r}_i)\right]$$
$$+(\hat{G}\boldsymbol{E}_\mathrm{in}(0))\exp(\mathrm{i}\boldsymbol{k}_0\boldsymbol{r}_i\tilde{n}_\mathrm{m}), \tag{20}$$

$$\boldsymbol{E}_\mathrm{refl}(\boldsymbol{R}) = \alpha_\mathrm{p}\sum_{j=1}^{S}[\hat{C}_\mathrm{p}^{+}(\boldsymbol{R}-\boldsymbol{r}_j)]'\boldsymbol{E}_{j\,\mathrm{eff}}(\boldsymbol{r}_j)$$
$$+(\hat{R}\boldsymbol{E}_\mathrm{in}(0))\exp(\mathrm{i}\boldsymbol{k}_0\boldsymbol{R}), \tag{21}$$

where $\hat{C}_\mathrm{p}^{+}$ takes place when the observation point is 'above' the layer (the field radiates in the positive direction of the z axis), while $\hat{C}_\mathrm{p}^{-}$ takes place when the observation point is 'below' the layer (the field radiates in the negative direction of the z axis).

Let us study the optical response of the system under consideration. Note that each solution of the system of equations (20), (21) does not characterise the optical field of the chaotic system even if the coordinates of the particles within one domain are distributed chaotically, but allows one to find $\boldsymbol{E}_\mathrm{refl}(\boldsymbol{R})$ for the given quasi-ordered structure. To eliminate this obstacle, we will average the results of some numerical experiments for different geometries of the system, generated by a random number generator. We will determine the necessary number of calculations based on the requirement of the stability of the mathematical expectation with an accuracy specified *a priori*.

5.1. Comparison of the Maxwell-Garnett effective medium with the theory

One of the most often used effective-medium theories is the Maxwell-Garnett theory [10, 14, 19], which allows the effective dielectric constant of the nanocomposite to be written in the form [10, 18, 38]:

$$\tilde{\varepsilon}_\mathrm{eff} = \tilde{\varepsilon}_\mathrm{m}\frac{(\tilde{\varepsilon}+2\tilde{\varepsilon}_\mathrm{m})+2\eta(\tilde{\varepsilon}-\tilde{\varepsilon}_\mathrm{m})}{(\tilde{\varepsilon}+2\tilde{\varepsilon}_\mathrm{m})-\eta(\tilde{\varepsilon}-\tilde{\varepsilon}_\mathrm{m})}, \tag{22}$$

where η is the factor of medium filling with particles (the ratio of the total volume of particles to the medium volume). As was mentioned above, this approach has some serious limitations [38] resulting from the use of electrostatic approximation and from averaging of the parameters over the volume. Nevertheless, in the case of small concentrations of nanoparticles, this approach yields results, in agreement with the experimental data. In this connection, it will be interesting to compare the optical response of a chaotic composite medium calculated within the approach proposed in this paper with the calculations obtained with the help of expression (22). Because the relationship derived by Maxwell-Garnett is independent of the size of nanoaggregates composing a cluster and the effective dielectric constant of the medium is determined by the filling factor, we will average $\boldsymbol{E}_\mathrm{refl}(\boldsymbol{R})$ from (21) not only over different geometries but also over different sizes of the particles, which meet, however, the long-wave condition (2).

Figure 2 presents the results of calculations for glass films with different volume concentrations of the particles. Good agreement obtained within the framework of the proposed method and Maxwell-Garnett theory, as is expected, takes place at sufficiently small nanoparticle concentrations (see Fig. 2a) when only the terms proportional to k_0^2/R [see (6)] are significant in the expansion of fields scattered by nanoparticles. The role of the terms proportional to $\mathrm{i}k_0/R^2$ and $1/R^3$ increases with increasing η. Thus, for example, the distance between the centres of nanoinclusions in Fig. 2c amounts to (2.2–2.4)a, where

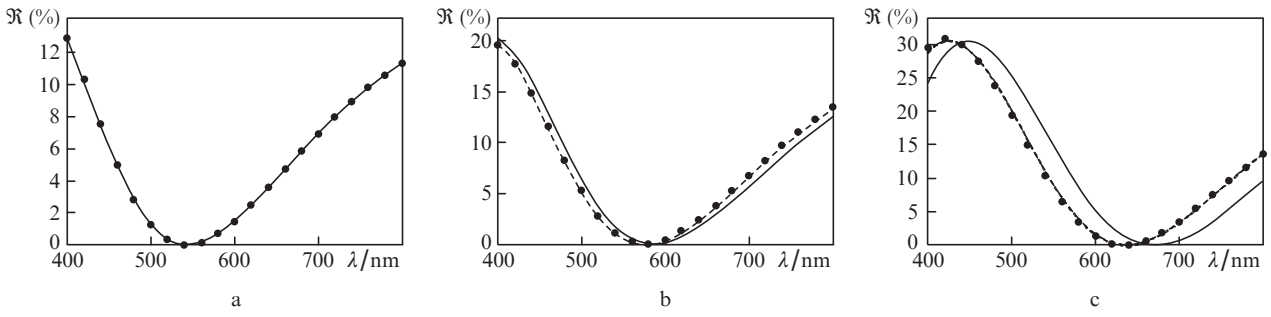

Figure 2. Reflectivity ℜ of the composite film of thickness h = 180 nm, calculated within the framework of the proposed theory (dots) and Maxwell-Garnett theory (solid and dashed curves) at η = 0.01 (a), η = 0.15, h' = 177 nm (b) and η = 0.41, h' = 171 nm (c). The solid curves are the results of calculations for h, dashed curves – for h'. The medium-matrix is glass with $\tilde{n}_\mathrm{m}$ = 1.5 and n = 2.5; the angle of incidence of an external wave is hereafter treated as normal.

a is the particle radius and the ratio $(1/R^3)/(k_0^2/R) \approx 2-6$ in the visible wavelength range. In this case, the discrepancy between the dependences increases and manifests itself in the change of the spectral position of the reflection minimum.

The mentioned discrepancies can be however easily explained using the following assumptions. The position of the minimum on the wavelength scale is determined (with account for the phase shift by π upon reflection from the upper boundary) by the interference quenching condition $hn_{\text{eff}} = \lambda/2$, where h is the film thickness. To this end, the best agreement between the proposed method and effective-medium theory can be achieved if

$$hn_{\text{eff}\,1} = hn_{\text{eff}\,2}, \tag{23}$$

where $hn_{\text{eff}\,1,2}$ are the effective refractive indices of the film, the indices being calculated with the help of the discussed methods. Varying the film thickness within the framework of the Maxwell-Garnett theory, we obtain the best agreement between the dependences at $h' = 177$ nm (Fig. 2b, dashed curves) and $h' = 171$ nm (Fig. 2c, dashed curves). It follows herefrom that the medium obtained by using the integral averaging of the parameters over the volume (within the framework of the Maxwell-Garnett theory – the effective medium) is more optically dense than the medium with chaotically distributed nanoinclusions, the difference being the higher the larger the filling factor. Indeed, it is known that reflection from a single nanoparticle layer is weaker than from a film of the same thickness having the dielectric constant calculated in accordance with (22) [39].

5.2. Comparison with the exact numerical calculation

We will test the proposed approach by comparing it with the exact numerical solution of Maxwell's equations with the help of the finite element method [23, 40]. To do this, we will consider the reflection spectrum of the composite film with an ordered distribution of nanoparticles. Ordering the nanoinclusions necessitates from the complexity of the finite element method, which makes it of little use for simulation of a chaotic structure [23]. On the other hand, the correctness of derived expressions (20), (21) with allowance for all the introduced approximations can be confirmed in an obvious way if we compare the results obtained for an ordered nanocomposite system once the latter is described by the same relations as the chaotic one.

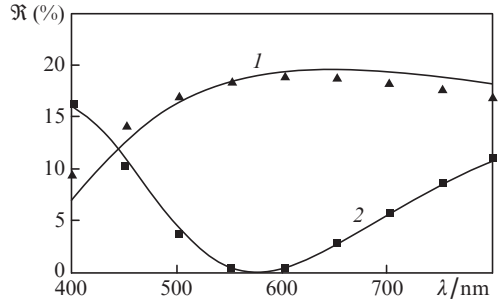

Figure 3. Reflectivity ℜ of the composite film implanted with three ordered layers of nanoparticles (the upper and lower layers are located close to the film boundaries). The points are the results of numerical calculations by the finite element method, the solid curves are the results of calculations by the proposed method. The parameters of the system: $h = 100$ nm, $a = 15$ nm, the interparticle distance inside the layer is $3a$, the interlayer distance is $4a$ (*1*), and $h = 180$ nm, $a = 15$ nm, the interparticle distance inside the layer is $4a$, the interlayer distance is $5a$ (*2*). The medium-matrix is glass with $\tilde{n}_{\text{m}} = 1.5$ and $n = 2.5$.

Figure 3 shows the calculated spectral dependences of the reflection coefficient for two glass films implanted with three single layers of ordered nanoparticles. Obviously, the obtained results are in good agreement with the rigorous solution; this confirms the applicability and accuracy of the proposed method for simulating the optical properties of nanocomposite films. Moreover, because within the framework of the finite element method nanoinclusions are characterised not by microscopic values, as is the case in equation (1), but by a macroscopic dielectric constant of the material used in films, the consistency of the calculation data also confirms the validity of transformation (5), which makes it possible to pass to macroscopic description of both dielectric and conducting nanoparticles.

Note that the interparticle distance in the ordered aggregates under study is such (see the caption to Fig. 3) that the terms proportional to ik_0/R^2 and $1/R^3$ as well as delayed electrodynamic interaction play an important role in the expansion of the field scattered by the particles (6); these terms and interaction, as follows from the results presented in Fig. 3, are adequately taken into account within the framework of the proposed model. Investigation of this composite (or chaotic composite with the same average interparticle distance) within the framework of the Maxwell-Garnett effective-medium theory will inevitably yield an error because this theory does not take into account the mentioned effects.

It should be emphasized that we mentioned in [21, 22] good agreement of calculated spectra of single layers of nanoparticles in vacuum or on the substrate surface with the exact results obtained by the finite element method.

5.3. Size dependence of the optical properties of a chaotic nanoaggregate

We will study the dependence of the optical response of the system under consideration on the nanoparticle size. As a material for the particles, we will use gold whose dispersion dependences $\tilde{\varepsilon}(\omega)$ are well known [41], and will take into account the size corrections to the dielectric constant of solid gold, which appear by limiting the mean free path of conduction electrons in a nanocluster [38]. To this end, we will use the Drude model [38, 42] for which the optical constants of a small metal particle can be written in the form:

$$\tilde{\varepsilon}'(\omega) = \tilde{\varepsilon}(\omega) + \frac{\omega_{\text{pl}}^2}{\omega(\omega + \mathrm{i}\gamma_b)} - \frac{\omega_{\text{pl}}^2}{\omega(\omega + \mathrm{i}\gamma_b')},$$
$$\gamma_b' = \gamma_b + \frac{0.7 v_{\text{F}}}{a}, \tag{24}$$

where $\omega_{\text{pl}} = 1.297 \times 10^{16}$ rad s^{-1} is the plasma frequency; $\gamma_b = 1.297 \times 10^{16}$ s^{-1} is the decay constant of solid gold; v_{F} is the Fermi velocity of free electrons.

We will keep the filling factor constant ($\eta = 0.2$) and will vary the radius a of particles and their number S in the domain by using the explicit relation

$$\eta = \frac{4\pi}{3}\frac{a^3 S}{d^2 h}.$$

As a medium-matrix, we will use vacuum for simplicity.

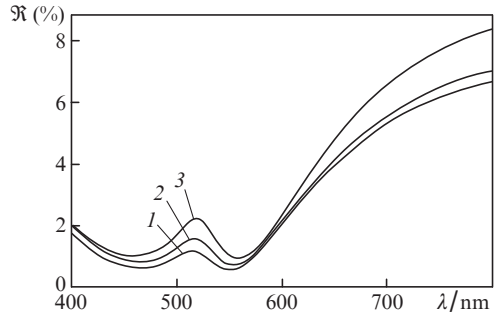

Figure 4. Reflectivity ℜ of the composite film with chaotically distributed gold nanoparticles of radii a = 12, (*1*), 15 (*2*), and 20 nm (*3*). The aggregate parameters are h = 200 nm, $\eta = 0.2$, $\tilde{n}_{\rm m} = 1$.

Figure 4 presents the spectral dependences of the reflectivity of the composite structure made of nanoclusters with three different radii. It is obvious that apart from a quantitative change in the curves, which is caused by an increase in the absolute value of the reflectivity, we also deal with a qualitative change, which manifests itself as a shift of a plasmon peak towards longer wavelengths when the particle radius increases (see Fig. 5). To explain this effect, we will use the effective polarisability formalism [21, 22].

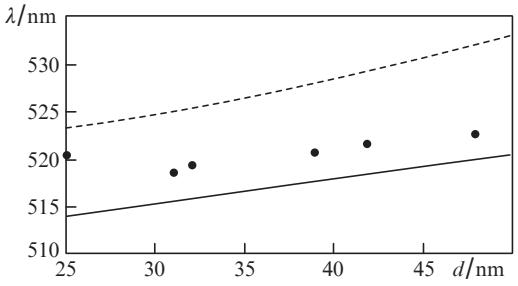

Figure 5. Position of the plasmon peak in a system of gold nanoparticles as a function of their diameter. The aggregate parameters are h = 200 nm, $\eta = 0.2$, $\tilde{n}_{\rm m} = 1$. The solid line is the calculation by the proposed method, the dashed curve is the calculations by the interpolation function from [38], and points are the experimental data [42].

We will write the explicit relation

$$\boldsymbol{d}_{\rm p} = \alpha_{\rm p}\boldsymbol{E}_{\rm eff} = \hat{\alpha}_{\rm p\,eff}\boldsymbol{E}_{\rm in}, \tag{25}$$

where $\boldsymbol{d}_{\rm p}$ is the dipole moment of a nanocluster. At $\tilde{n}_{\rm m} = 1$, expressions (20) and (25) allow us to obtain an expression for the effective polarisability of particles of the ith layer:

$$\hat{\alpha}_{{\rm p}i\,{\rm eff}} = \frac{\alpha_{\rm p}}{1 - \alpha_{\rm p}\hat{A}_{\rm p}} \times\left[\exp({\rm i}\boldsymbol{k}_0\boldsymbol{r}_i) + \alpha_{\rm p}\sum_{j=1,j\neq i}^{S}\frac{\boldsymbol{E}_{j\,{\rm eff}}(\boldsymbol{r}_j)}{\left|\boldsymbol{E}_{\rm in}(0)\right|}\hat{C}_{\rm p}^{\pm}(\boldsymbol{r}_i - \boldsymbol{r}_j)\right]. \tag{26}$$

In this case, the frequency dependence of $(\tilde{\varepsilon} - 1)/(\tilde{\varepsilon} + 2)$ [entering (5) and determining polarisability $\alpha_{\rm p}$ of the cluster] exhibits, according to experimental data [41], a markedly pronounced resonance behaviour and can be approximated by the resonance frequency function. As a result, the polarisability takes the form:

$$\alpha_{\rm p} = a^3\left(\frac{A}{\omega_0 - \omega + {\rm i}\Gamma}\right), \tag{27}$$

where ω_0 is the resonance frequency; A and Γ are the amplitude and relaxation constants. Thus, expression (26) transforms to the form:

$$\hat{\alpha}_{{\rm p}i\,{\rm eff}} = \frac{Aa^3}{\omega - \omega_0' + {\rm i}\Gamma'} \times\left[\exp({\rm i}\boldsymbol{k}_0\boldsymbol{r}_i) + \alpha_{\rm p}\sum_{j=1,j\neq i}^{S}\frac{\boldsymbol{E}_{j\,{\rm eff}}(\boldsymbol{r}_j)}{\left|\boldsymbol{E}_{\rm in}(0)\right|}\hat{C}_{\rm p}^{\pm}(\boldsymbol{r}_i - \boldsymbol{r}_j)\right], \tag{28}$$

where $\omega_0' = \omega_0 - Aa^3\,{\rm Re}[\hat{A}_{\rm p}]$ is the shifted resonance frequency; $\Gamma' = \Gamma - Aa^3\,{\rm Im}[\hat{A}_{\rm p}]$. Therefore, the plasmon resonance frequency (and accordingly the wavelength) will change proportionally to a change in the particle radius. An increase in the amplitude of the scattered field proportional to the effective polarisability of the particles is also obvious.

Note that the exact shape of these dependences will depend on the solution of equations (20)–(28), the type of interpolation function (27), and the contribution of the size correction (24); these presented assumptions are of explanatory character. It should be also emphasised that the most widely used effective-medium theories, such as the theories put forward by Maxwell-Garnett, Clausius–Mosotti, etc. [38], take into account only the filling factor and neglect the size of the particles.

The dependence (repeatedly studied experimentally [38, 42, 43], and in the case of a particle – theoretically) of the plasmon peak position on the cluster size was predicted within the known Mie theory [17, 18]. Figure 5 shows the dependence of the plasmon peak position, calculated by the proposed method (solid line) and obtained in experiments (points) in [42]. Note that the experimentally found wavelengths, which correspond to the position of plasmon peaks of gold particles with various radii, differ. For example, Khlebtsov [38] analysed dozens of papers devoted to this problem and showed that the particle diameter corresponding to the peak at one or other wavelength can vary by 1.5–1.8 times from paper to paper. According to Khlebtsov and some other works being analysed, this spread is caused by polydispersion and polymorphism of the clusters under study, which in turn results from specific character of production of nanoparticles of the required size. To this end, nanoparticles with a shape closest to spherical and with a high degree of monodispersion were obtained in paper [42]; therefore, it is reasonable to compare the calculated dependences with the results of paper [42]. Figure 5 also presents the interpolation dependence (dashed curve) obtained in [38] by averaging the experimental results of 15 papers. This curve in view of the above-mentioned reasons (polydispersion of the colloids under study and deviation from the spherical shape of colloid particles) differs both from the results of [42] and from the calculated curve plotted within the framework of the proposed model. Note that this discrepancy does not demonstrate the invalidity of our approach because we performed calculations for monodisperse systems consisting of ideally spherical particles and, as is seen from Fig. 5, the theoretical results are in good agreement with experimental data [42], where (as was noted above) the effect of polymorphism and polydispersion was noticeably reduced.

6. Conclusions

Thus, we have proposed in this paper the microscopic effective-medium theory which allows us to study composite nanostructures with a different degree of structural order. The proposed approach makes it possible to calculate the optical parameters of dense aggregates where the effects of interaction of nonadjacent particles are significant. Because the method interprets the heterogeneous medium microscopically, it is possible to take into account such peculiar features of nanoparticles as shape, size, etc. We have shown that at small concentrations of nanoparticles, the results of the Maxwell-Garnett theory well agree with the results of calculations performed within the proposed method (see Fig. 2a). The discrepancy between the results increases with increasing nanoparticle concentration because averaging the parameters within the integral theory yields overestimated values of the effective optical density of the film. Comparison of the results of the proposed approach with those of exact numerical calculations for an ordered nanoaggregate demonstrates their good agreement. The studied dependence of the optical response of the composite film on the size of implanted metal nanoparticles is also consistent with the experimental data.

References

1. Shalaev V.M., Wenshan Cai, Uday K. Chettiar, et al. *Opt. Lett.*, **30**, 3356 (2005).
2. Smith D.R., Pendry J.B. *J. Opt. Soc. Am. B.*, **23**, 391 (2006).
3. Agranovich V.M., Shen Y.R., Baughman R.H., et al. *Phys. Rev. B*, **69**, 165112 (2004).
4. Gadomskii O.N., Shalin A.S. *Zh. Eksp. Teor. Fiz.*, **132**, 870 (2007).
5. Li Z.M., Liu H.J., Ye J.T., et al. *Appl. Phys. A*, **78**, 1121 (2004).
6. Liu X., Pichler T., Knupfer M., et al. *Phys. Rev. B*, **66**, 045411 (2002).
7. Gadomskii O.N., Shalin A.S. *Fiz. Met. Metalloved.*, **101**, 462 (2006).
8. Grigorenko A.N., Geim A.K., Gleeson H.F., et al. *Nature*, **438**, 335 (2005).
9. Zhang S., Fan W., Panoiu N.C., et al. *Phys. Rev. Lett.*, **95**, 137404 (2005).
10. Sukhov S.V. *Kvantovaya Elektron.*, **35**, 741 (2005) [*Quantum Electron.*, **35**, 741 (2005)].
11. Genet C., Ebbesen T.W. *Nature*, **445**, 39 (2007).
12. Alu A., Engheta N. *Phys. Rev. E*, **72**, 016623 (2005).
13. Garcia de Abajo F.J., Gomez-Santos G., Blanco L.A., et al. *Phys. Rev. Lett.*, **95**, 067403 (2005).
14. Maxwell-Garnett J.C. *Philos. Trans. R. Soc.*, **A203**, 385 (1904).
15. Shalin A.S. *Zh. Prikl. Spektrosk.*, **73**, 641 (2006).
16. Oraevsky A.N., Protsenko I.E. *Kvantovaya Elektron.*, **31**, 252 (2001) [*Quantum Electron.*, **31**, 252 (2001)].
17. Mishchenko M.I., Travis L.D., Lacis A.A. *Scattering, Absorption and Emission of Light by Small Particles* (Cambridge: Cambridge Univ. Press, 2002).
18. Bohren C., Huffman D. *Absorption and Scattering of Light by Small Particles* (New York: Wiley, 1983; Moscow: Mir, 1986).
19. Moiseev S.G., Pashinina E.A., Sukhov S.V. *Kvantovaya Elektron.*, **37**, 446 (2007) [*Quantum Electron.*, **37**, 446 (2007)].
20. Shalin A.S. *Izv. Vyssh. Uchebn. Zaved. Ser. Fiz.*, **49**, 3 (2006).
21. Shalin A.S., Moiseev S.G. *Opt. Spektrosk.*, **106**, 1029 (2209).
22. Shalin A.S., *Pis'ma Zh. Eksp. Teor. Fiz.*, **90**, 279 (2009).
23. Arfken G.B., Weber H.J. *Mathematical Methods for Physicists* (New York: Acad. Press, 1995).
24. Taflove A., Hagness S.C. *Computational Electrodynamics: The Finite-Difference Time-Domain Method* (Boston: Artech House, 2000).
25. Prather D.W., Shi S. *J. Opt. Soc. Am. A.*, **16**, 1131 (1999).
26. Yurkin M.A., Maltsev V.P., Hoekstra A.G. *J. Quant. Spectr. & Rad. Transf.*, **106**, 546 (2007).
27. Sukhov S., Haefner D., Dogariu A. *Phys. Rev. E*, **77**, 066709 (2008).
28. Born M., Wolf E. *Principles of Optics* (Oxford: Pergamon Press, 1975).
29. Khlebtsov B.N., Melnikov A.G., Zharov V., et al. *Nanotechnol.*, **17**, 1437 (2006).
30. Sakoda K. *Optical Properties of Photonic Crystals* (Berlin: Springer, 2005).
31. Sukhov S.V., Krutitsky K.V. *Phys. Rev. B*, **65**, 115407 (2002).
32. Born M. Huang T. *Dynamic Theory of Crystal Lattices* (Oxford: Clarendon, 1956; Moscow: Inostr. Lit., 1958).
33. Poppe G.P.M., Del Sole R., Manghi F. *Phys. Rev. B*, **44**, 1825 (1991).
34. Draine B.T., Flatau P.J. *J. Opt. Soc. Am. A*, **11**, 1491 (1994).
35. Poppe G.P.M., Wijers C.M.J., Silfhout A. *Phys. Rev. B*, **44**, 7917 (1991).
36. Wijers C.M.J., Poppe G.P.M. *Phys. Rev. B*, **46**, 7605 (1992).
37. Moroz A. *Phys. Rev. B*, **66**, 115109 (2002).
38. Khlebtsov N.G. *Kvantovaya Elektron.*, **38**, 504 (2008) [*Quantum Electron.*, **38**, 504 (2008)].
39. Milton G.W. *The Theory of Composites* (Cambridge: Cambridge Univ. Press, 2004).
40. COMSOL Multiphysics 3.4, COMSOL AB, Stockholm, Sweden; http://www.comsol.com/products/multiphysics/.
41. Johnson P.B., Christy R.W. *Phys. Rev. B*, **6**, 4370 (1972).
42. Andreescu D., Sau T.K., Goia D.V. *Colloid Interface Sci.*, **298**, 742 (2006).
43. Bogatyrev V.A., Dykman L.A., Khlebtsov B.N., et al. *Opt. Spektrosk.*, **96**, 139 (2004).